

Monte-Carlo Sphere Model for "Effective Oxide Thinning" Induced Extrinsic Breakdown

Huan-Tsung Huang, Ming-Jer Chen, Jyh-Huei Chen

Department of Electronics Engineering, National Chiao-Tung University, Hsin-Chu 300, Taiwan, R.O.C.

Tel: 886-3-5712121 ext. 54217 Fax: 886-3-5723016 E-mail: mjchen@bicmos.ee.nctu.edu.tw

Chi-Wen Su, Chin-Shan Hou, Mong-Song Liang

R&D Department, Taiwan Semiconductor Manufacturing Company, Hsin-Chu 300, Taiwan, R.O.C.

Abstract

Monte-Carlo sphere model is further extended to the extrinsic time-dependent-dielectric-breakdown (TDDDB) by incorporating the well-known "effective oxide thinning" concept. This paper demonstrates for the first time that the defect-related extrinsic TDDDB is also statistics in nature as the intrinsic one, and is characterized by the defective area and the effective thickness as well as their probability density defining a specific defect size used in simulation. The experimental bimodal or even multi-modal characteristics can be adequately reproduced in terms of these parameters. Furthermore, the Monte-Carlo simulation in the extrinsic regime is found to be sample size related, suggesting that care should be taken when evaluating extrinsic TDDDB data in a real manufacturing process.

Introduction

The time-dependent-dielectric-breakdown (TDDDB) of thin oxides is one of the major reliability issues in scaled CMOS technologies. The oxide wearout can be regarded as a process of the electron trap generation during stress, eventually leading to a breakdown event. Recently, a Monte-Carlo (MC) sphere model for this trap generation process has successfully explained and reproduced the experimentally observed thickness and area effects [1],[2]. However, their simulations had not dealt with the extrinsic TDDDB that is far more important in a real manufacturing process concerning the early failure. This paper for the first time incorporates the "effective oxide thinning" concept [3] into the MC sphere model. As a result, the extrinsic or "B" mode characteristics can be reproduced with a clear picture of defective severity and its uniformity across the wafers and lots.

MC Sphere Percolation Simulation

A MC sphere percolation simulation program [2] based on the algorithm addressed in [1] is adopted for both intrinsic and extrinsic TDDDB. Unless stated elsewhere, the TDDDB is represented by the critical electron trap density N_T which triggers the breakdown event as explained in [1],[2]. The schematic diagram is shown in Fig. 1. Fig. 2 shows the simulated intrinsic TDDDB distributions for different oxide thicknesses down to $t_{OX} = 1.6$ nm. These distribution lines tend to saturate for $t_{OX} > 2.5$ nm as can be seen more clear in terms of modal values in Fig. 3. Such saturation behavior is consistent with the ultimate thickness limit for breakdown [4]. As to the extrinsic MC simulation, first we set effective oxide thinning Δt_{OX} to a fixed value in all trials. The results are shown to be shifted, with the accompanying change in slope, from the intrinsic case in Fig. 4 (a) and (b) for $t_{OX} = 4$ and 6 nm, respectively. That means that all samples with the same quality exhibit no bimodal characteristics, even though the areas of the "effective defects" are only $\sim 10\%$ of the total areas. Further looking into Fig. 5, the modal value decreases drastically until the effective ultimate thickness limit is encountered as revealed in Fig. 2 and 3.

The area A_D and thinning Δt_{OX} of the "effective defects" can both be randomly generated. In other words, the feature size of the "effective defects" varies among samples and are described by the probability density function. However, in this paper, only Δt_{OX} is treated as a random variable for simplicity. Probability density versus Δt_{OX} with sample size or trial number of 30,000 is shown in Fig. 6. The randomly generated

Δt_{OX} agrees well with the analytical expression: $\exp(b \cdot \Delta t_{OX})$ where b is responsible for the slope of the distributions. Both the randomly generated and calculated Δt_{OX} are normalized to the corresponding values with $\Delta t_{OX} = 0$. Also in this figure, $\Delta t_{OX,MAX}$ denotes the possible maximum effective oxide thinning. The simulation results with $b = -1.6, -1.1$, and -0.6 nm⁻¹ are shown in Fig. 7 for $t_{OX} = 6$ nm, $\Delta t_{OX,MAX} = 5$ nm, and sample size of 3,000. The bimodal characteristics are successfully produced with a clear picture of defective status among samples. Fig. 8 illustrates how the sample size influences the extrinsic distributions. $b = -0.6$ nm⁻¹ for all cases in this figure. It is clear that sample size affects significantly the distributions only for thinner $\Delta t_{OX,MAX}$ of 3 nm. Note that for $\Delta t_{OX,MAX} = 5$ nm the magnitude -4.5 in Weibull scale at $N_T = 10^{19}$ cm⁻³ corresponds to a cumulative percentage F of about $\frac{1}{91}$, indicating that the sample size of either 3,000 or 30,000 is much larger than 91. Thus, a stable, reliable distribution results. On the other hand, for $\Delta t_{OX,MAX} = 3$ nm, the results show the sample-size-limited characteristics. Again, -8 and -10 in Weibull scale at $N_T = 10^{19}$ cm⁻³ correspond to cumulative percentages F of about $\frac{1}{2,980}$ and $\frac{1}{22,000}$, respectively. In real world, it is not easy to have sample size large enough to reflect all kinds of defective status correctly. Therefore, the extrinsic TDDDB data in real manufacturing processes should be carefully interpreted. Experimental results can be compared between each other only under the same sample size with all data from above the certain value in Weibull scale.

Experiment and Comparisons

The test devices in our work were fabricated in a 0.25 μ m CMOS process with different oxide growth techniques (set 1) and with different areas (set 2). Set 1 and 2 were from different lots. Data were fitted as explained in the caption of Fig. 9. The fitting parameters of set 1 devices are $b = -3.1$ nm⁻¹ and $\Delta t_{OX,MAX} = 3$ nm, and $b = -0.8$ nm⁻¹ and $\Delta t_{OX,MAX} = 1.35$ nm for gate oxides grown in wet and dry O₂ ambient, respectively. $A_D/A_{OX} = 1/9$ as well. For both devices of set 2, $b = -0.3$ nm⁻¹, $\Delta t_{OX,MAX} = 0.8$ nm and $A_D/A_{OX} = 1/18$. Fitting of DryO(1)A device with alternative parameters of $b = -2.4$ nm⁻¹ and $\Delta t_{OX,MAX} = 2.2$ nm is shown in Fig. 9(b). As explained earlier, parameters used in Fig. 9(a) evaluates the experimental data better than those in Fig. 9(b).

Conclusion

Monte-Carlo sphere model is for the first time extended and successfully reproduces experimental extrinsic TDDDB. The sample-size limited characteristics clarified by the improved model suggest that care be highly taken when evaluating extrinsic TDDDB data in a real manufacturing process.

References

- [1] R. Degraeve, et al., *IEDM Tech. Dig.*, pp. 863-866, 1995.
- [2] H. T. Huang, et al., *International Symposium on VLSI Technology, Systems and Applications*, accepted for publication, 1999.
- [3] K. F. Schuegraf, et al., *IEEE Trans. Electron Devices*, Vol. 41, pp. 761-767, 1994.
- [4] D. J. DiMaria, et al., *Appl. Phys. Lett.*, Vol. 71, pp. 3230-3232, 1997.

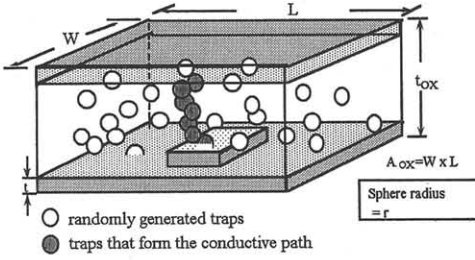


Fig. 1 The three-dimensional oxide structure on which the sphere-based Monte-Carlo percolation simulation is performed for breakdown. The transition region t accounts for the strained layer ($=0.5$ nm). The effective oxide thinning cubic has an area A_D and thickness Δt_{ox} . $A_{ox} = 30 \times 30$ nm² for simulation.

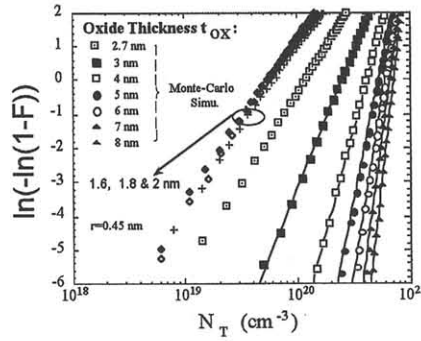


Fig. 2 Monte-Carlo simulation in intrinsic mode ($\Delta t_{ox}=0$). The distribution lines tend to saturate for the oxide thickness less than around 2.5 nm. Also shown (lines) are the calculation results from the published model [2].

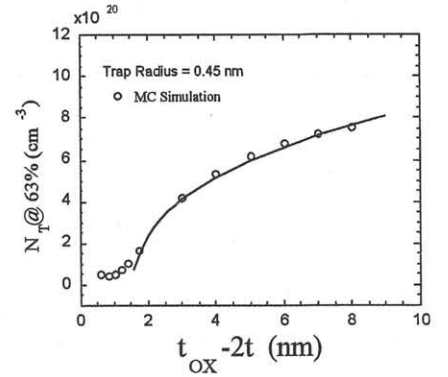


Fig. 3 Modal values of N_T versus oxide thickness minus $2t$ for trap radius $r=0.45$ nm in Monte-Carlo simulation. The ultimate thickness limit is clearly seen.

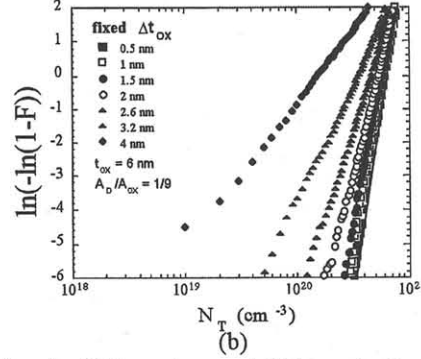
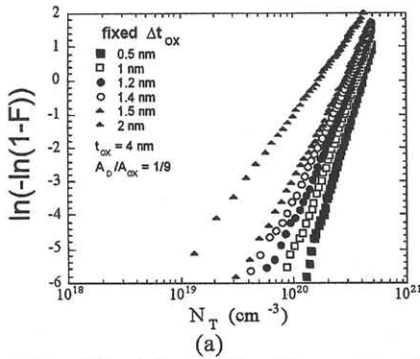


Fig. 4 Simulation results with respect to fixed Δt_{ox} for (a) $t_{ox} = 4$ nm and (b) $t_{ox} = 6$ nm. According to the results, the oxide thinning causes not only a shift but also a change in slope of the distributions. No bimodal characteristics are seen for the cases of fixed Δt_{ox} .

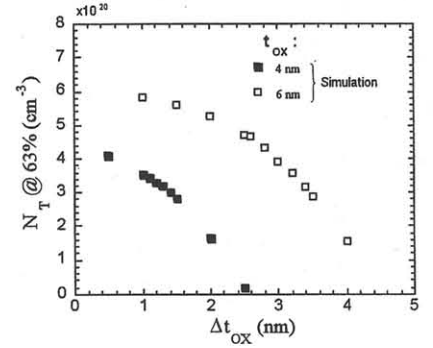


Fig. 5 Modal values of N_T versus fixed Δt_{ox} corresponding to Fig. 4.

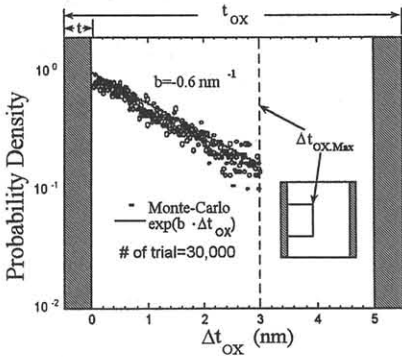


Fig. 6 Probability density distribution generated in the Monte-Carlo simulation, compared to the designated expression $\exp(b \cdot \Delta t_{ox})$. It is clear that a trial number of 30,000 exhibits good uniformity and follows the expression well.

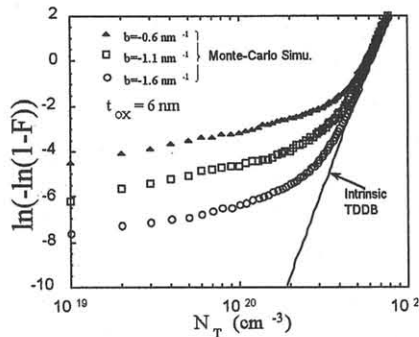


Fig. 7 Simulation results with respect to three different b 's. The smaller the absolute value of b , the bigger the (percentage) the samples with large oxide thinning. Here, $\Delta t_{ox,Max}$ and A_D are 5 nm and 100 nm², respectively.

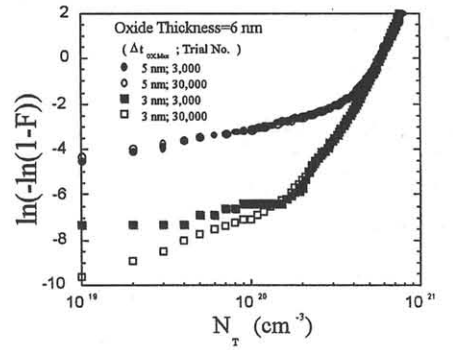
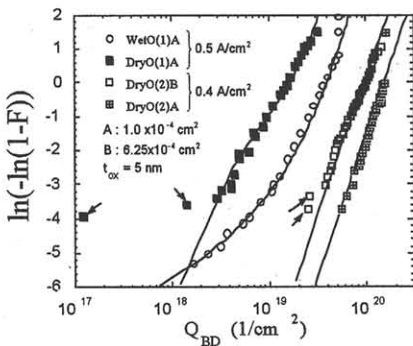
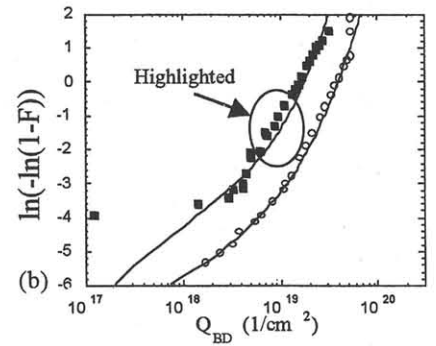


Fig. 8 Sample size or trial number limited characteristics of the extrinsic breakdown. The trustability of the extrinsic distribution is strongly related to the sample size as well as its corresponding value in Weibull scale.



(a)

Fig. 9 Comparison between charge-to-breakdown experiments (symbols) and calculations (lines), showing in part nice reproduction by the Monte-Carlo percolation simulation. The arrows in (a) indicate the data points that could be suffered from sample size limited problem. In (b), alternative fitting parameters are chosen to include more data points at the sacrifice of deviation in the medium Q_{BD} regime for DryO(1)A under 0.5 A/cm² stress.



(b)